

EZIGen: Enhancing zero-shot personalized image generation with precise subject encoding and decoupled guidance

Zicheng Duan¹, Yuxuan Ding², Chenhui Gou³, Ziqin Zhou¹, Ethan Smith⁴, Lingqiao Liu^{1,†}
 University of Adelaide¹, Xidian University², Monash University³, Leonardo.AI⁴
 {firstname.lastname}@{adelaide.edu.au}¹, yxding@stu.xidian.edu.cn²,
 chenhui.gou@monash.edu³, ethan@leonardo.ai⁴

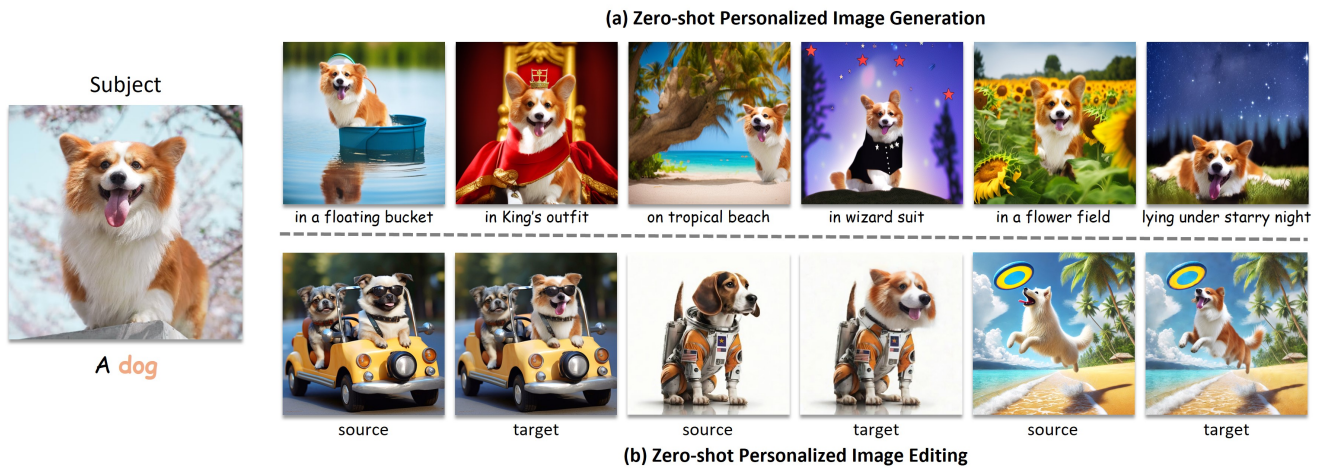


Figure 1. Our model demonstrates remarkable zero-shot performance in producing high-quality and flexible images from a single reference object and can serve as a versatile model for both personalized image generation and editing with a unified design.

Abstract

Zero-shot personalized image generation models aim to produce images that align with both a given text prompt and subject image, requiring the model to effectively incorporate both sources of guidance. However, existing methods often struggle to capture fine-grained subject details and frequently prioritize one form of guidance over the other, resulting in suboptimal subject encoding and an imbalance in the generated images. In this study, we uncover key insights into achieving high-quality balances on subject identity preservation and text-following, notably that 1) the design of the subject image encoder critically influences subject identity preservation, and 2) the text and subject guidance should take effect at different denoising stages. Building on these insights, we introduce a new approach, EZIGen, that employs two main components: a carefully crafted subject image encoder based on the pre-trained UNet of the Stable Diffusion model, following a process that balances the two guidances by separating their dominance stage and revisiting certain time steps to boot-

strap subject transfer quality. Through these two components, EZIGen achieves state-of-the-art results on multiple personalized generation benchmarks with a unified model and 100 times less training data. Demo Page: [Demo](#).

1. Introduction

Personalized image generation methods enable users to create images by combining text prompts with subject images, following the principle of ‘my subject’ following ‘my instructions’. Existing solutions fall into two categories: test-time tuning-based [1, 11, 13, 19, 20, 32] and zero-shot inference-based [7, 28, 30, 39]. Test-time tuning involves fine-tuning model parameters and introducing subject tokens, allowing detailed control but requiring time-consuming re-training. In contrast, zero-shot methods generate images directly from the given subjects without re-training, offering greater efficiency. This paper focuses on improving zero-shot methods.

Existing zero-shot methods [7, 28, 30, 39] predominantly focus on the transfer of a reference subject’s appear-



Figure 2. **Suboptimal subject encoding.** BootPIG’s encoder design may lead to degraded performance compared to ours.

ance into the generated image. These methods typically first encode the subject image and then integrate the encoded features into the UNet of the diffusion model. There are several existing options for subject image encoders. ELITE [39] and Subject Diffusion [28] utilize CLIP image encoders, while AnyDoor [7] adopts DINOv2 to achieve better feature map extraction. However, these methods all fail to capture details of the subject image, leading to significant distortion compared to the subject image. Recently, BootPIG [30] employs a Reference UNet model [15] as a subject feature extractor for common objects, reasoning that the feature space of a UNet would be more aligned with the feature space used in image generation. Although this approach is reasonable, it leaves many design aspects unexplored, such as which timestep to use and detailed extractor model configuration. Following their steps, our research reveals that those aspects might have a big impact on the identity preservation capability, as shown in Fig. 2.

Another often overlooked challenge in existing methods is balancing the parallel user inputs: subject image and text prompt. Although these guidance appear to be independent—the subject image focuses on preserving identity and the text prompt directs the model to follow user instructions—they in fact frequently interfere with one another. For instance, as shown in Fig. 3, both the text prompt “a dog in police outfit” and the subject dog image define the dog’s appearance to some extent simultaneously. In such cases, prior works either prioritize identity preservation at the expense of text coherence [28], successfully follow the text but struggle to maintain subject identity [30], or perform suboptimally in both aspects [20, 39].

In this paper, we address the aforementioned challenges and Enhance Zero-shot personalized Image Generation by proposing a novel method called EZIGen. Firstly for subject encoding, we follow [30] to initialize a Stable Diffusion UNet as an extractor to achieve good feature alignment between the subject and generated images. However, our unique contribution lies in identifying the ‘devils in the details’: Different from [6, 15] that removes the time embed-

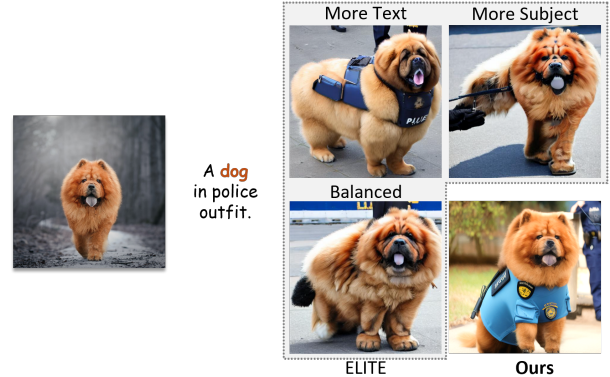


Figure 3. **Conflicting guidance.** Existing methods struggle to balance between identity preservation and text prompt alignment.

ding and fully-finetunes a Stable Diffusion UNet to serve as time-irrelevant Reference UNets and [30] where the Reference UNet is tuned and is synchronized with the denoising timesteps, we discover that simply adding noise and denoising the subject image to the final denoising step $T_1 \rightarrow 0$ with a vanilla frozen Stable Diffusion UNet yields significantly improved subject representations. Secondly, to better balance subject identity and text adherence, we decouple the generation process into two distinct stages: the Sketch Generation Process, which forms a coarse sketch latent from text prompts, and the Appearance Transfer Process, which injects the encoded subject details via the adapter. This decoupling explicitly separates guidance signals. Additionally, we observe that the sketch latent can impact the quality of appearance transfer—a sketch latent closer to the subject tends to produce better results. Therefore, we introduce an iterative pipeline that repeatedly converts the generated image back into the editable noisy latent to serve as a new sketch latent that ensembles more visual cues from the given subject, and progressively achieves satisfactory results as the iteration continues. With the aforementioned designs, our contribution can be summarized as follows: **1)** We identify that the design choices of the subject image encoder significantly impact identity preservation and propose an improved design over existing solutions. **2)** We propose a solution that combines guidance decoupling with iterative bootstrapping to address the guidance balance issue. **3)** We extend our approach to personalized image editing and domain-specific personalization tasks. **4)** Extensive experiments and analysis demonstrate the state-of-the-art performance of EZIGen.

2. Related Works

2.1. Text-to-image generation.

Generative models are designed to synthesize samples from a data distribution based on a set of training examples. These models include Generative Adversarial Networks (GANs) [4, 12, 16], Variational Autoencoders (VAEs) [17],

autoregressive models [10, 31, 35, 37], and diffusion models [3, 8, 14, 34]. While these approaches have demonstrated remarkable capabilities in generating high-quality and diverse images, their inputs are typically restricted to text prompts. In contrast, our work significantly enhances pre-trained diffusion models by enabling them to incorporate additional image guidance alongside text prompts, providing them with a wider range of applications and contexts.

2.2. Tuning-based personalized image generation.

Tuning-based personalized image generation [2, 5, 9, 11, 13, 19, 26, 29, 32] typically adjust sets of parameters to extend traditional text-driven methods, allowing them to incorporate additional subject images alongside text prompts. Some approaches focus on tuning text embeddings to represent the subject accurately, such as TextualInversion[11], which simply adjusts a learnable text embedding, and DreamBooth[32], which fine-tunes both text embeddings and model parameters for more precise and effective control. [13, 19] further improve performance by additionally tuning cross-attention layers, enhancing subject appearance integration. Despite these advancements, these methods require re-training for each individual subject, making them time-consuming, and unsuitable for productivity in large-scale applications or practical deployments.

2.3. Zero-shot personalized image generation

To tackle the aforementioned issues, some researchers introduced zero-shot methods that accept new subjects without requiring retraining. Some attempts [23, 33, 38, 40, 42], developed zero-shot personalized generation techniques for domain-specific data, such as human faces or other constrained applications. Recently, for more general objects, ELITE[39] pioneeringly projects the image into text space and refines with detailed patch features, BLIP-Diffusion[20] leverages a Q-Former[21] to align text and images, Subject-Diffusion[28] inject grounding info to control the subject position, BootPIG[30] setups a Reference UNet to extract subject features. Nevertheless, these methods struggle with issues like degraded subject-identity preservation due to sub-optimal feature extractor utilization or poor balancing between the text and subject guidance during the generation process.

3. Methods

Our method comprises two main components: a technique to encode the subject image for the generation process and a strategy to balance subject identity preservation with text alignment. We will first elaborate on these components for personalized image generation and then extend the discussion to personalized image editing.

3.1. Encoding and injecting subject feature

The identity information of the subject image is often extracted using an image encoder. Current methods use options like CLIP[28], DINO-V2[7]), or a Reference UNet[30] trained based on Stable Diffusion UNet. Leveraging a Stable Diffusion UNet for subject feature extraction is particularly appealing as it naturally aligns with the Stable Diffusion feature space, reducing the challenge of aligning disparate feature spaces. However, this design raises open questions about configuring the feature extractor and integrating subject encoding into the Stable Diffusion UNet. In BootPIG [30], all Reference UNet parameters are fine-tuned, with progressively noised input images fed at each timestep, allowing subject image features to be injected into its Main UNet for generation. However, we identify potential issues: overly-noised features may distort subject information, and tuning Stable Diffusion parameters into a Reference UNet can lead to suboptimal subject encoding, leading to degraded subject encoding(Fig. 2 shows some examples). In this paper, we propose a simple yet effective solution: First, we directly take the vanilla Stable Diffusion UNet and conduct one-step denoising on a one-step noised subject image to obtain intermediate subject feature maps from UNet as the subject appearance feature. Second, we again take the same UNet and insert cross-attention adapters in its transformer block to adopt the subject image guidance.

Specifically, we first initialize a pre-trained Stable Diffusion UNet, denoted as U . Unlike [6, 15, 30] that train a separate copy of Stable Diffusion UNet as Reference UNet, EZIGen requires only a *SINGLE FIXED COPY* of U during the entire procedure, reducing complexity and saving computational resources. Then to extract subject representations, as shown in the gray box in Fig. 4, we set the denoising timestep $t = 1$ and add random gaussian noise ϵ to the subject image latent I^{sub} , depending on the t^{sub} and a noise scheduler ϕ to perform a one-step noise addition:

$$I_{t=1}^{\text{sub}} = I^{\text{sub}} + \phi(\epsilon, t = 1), \epsilon \sim \mathcal{N}(0, \sigma^2) \quad (1)$$

This slightly noised image latent I^{sub} and the timestep t^{sub} are then passed to U to conduct a one-step denoise ($t^{\text{sub}} = 1 \rightarrow t^{\text{sub}} = 0$) and obtain the feature maps from all N self-attention layers, collectively denoted as \mathcal{F}^{sub} :

$$\mathcal{F}^{\text{sub}} = \{s_1, s_2, \dots, s_N\} = U(I_{t=1}^{\text{sub}}, t = 1) \quad (2)$$

Notably, we perform this extraction only ONCE throughout the entire generation process, and we set the extracted feature maps \mathcal{F}^{sub} as fixed offline feature maps for later utilization.

After obtaining the features, we insert an adapter as a trainable cross-attention module between the self-attention and cross-attention layers within each transformer block of

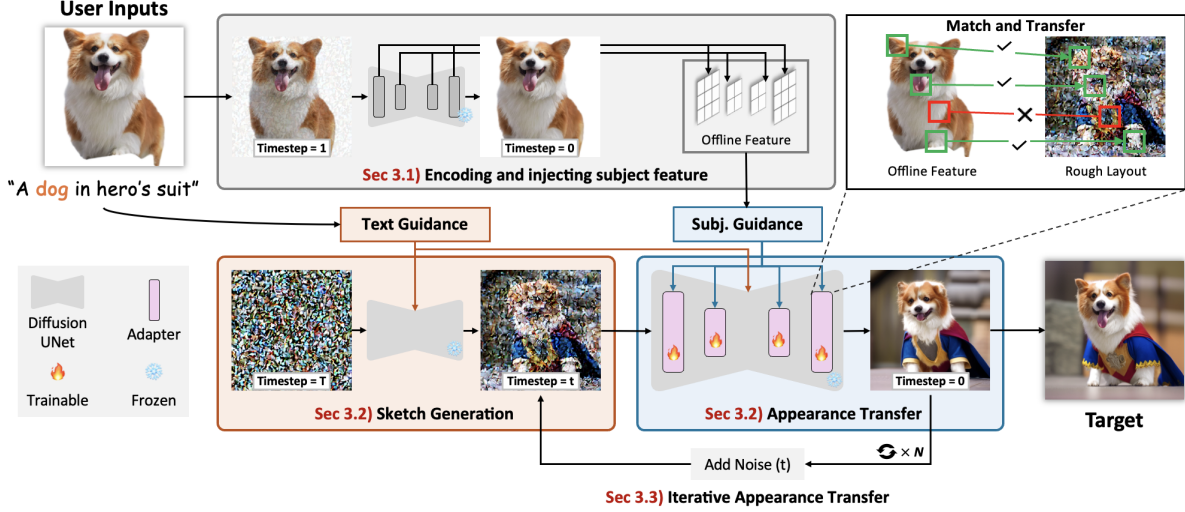


Figure 4. Illustration of the proposed system. We begin by Encoding and Injecting subject features (Sec. 3.1). Next, we decouple one generation process into the Sketch Generation Process and Appearance Transfer Process (Sec. 3.2). Finally, we introduce the Iterative Appearance Transfer mechanism (Sec. 3.3) to fully transfer the subject appearance feature to the sketch latent.

U , resulting in a total of N adapters. In each adapter A_n , the latent feature x_n from U is projected into query, key, and value matrices Q_n , K_n , and V_n respectively and the subject feature s_n is mapped into additional key K_n^{sub} and value V_n^{sub} tokens as follows:

$$K_n^{\text{sub}} = W_k s_n, \quad V_n^{\text{sub}} = W_v s_n \quad (3)$$

The output feature \mathcal{F}_n for each adapter A_n is then computed by combining the features from U with the subject features through the following attention operation:

$$\mathcal{F}_n = A_n(Q_n, [K_n \| K_n^{\text{sub}}], [V_n \| V_n^{\text{sub}}]) \quad (4)$$

Here, the $[\cdot \| \cdot]$ operator represents the concatenation of features along the token dimension.

Training. We only train the each adapter A_n to accept the subject appearance feature s_n and leave the UNet U intact. We follow standard practices in the field to construct image pairs from image/video datasets as training data. In each pair, one image serves as the subject, while the other is treated as the target. As such, the adapters transfer the subject appearance into the generation process and guide the model to recover the noisy target image.

3.2. Decoupling text and subject guidance

As mentioned previously, existing methods [28, 30, 39] often struggle to balance subject ID preservation, i.e. subject guidance, with text adherence, i.e. text guidance. While the design in Sec. 3.1 excels in preserving subject identity, it still faces challenges in achieving this balance as we observe that injecting subject features alongside text prompts at all timesteps tends to prioritize subject identity, overshadowing text-guided semantic and color patterns that are not fully established in the early stages. Instead of using parallel guidance with scaling factors [28, 30, 39], which often

compromises one aspect, we decouple the guidances to let them dominate at different stages: text guidance in the early stages and subject guidance details later. This leads to two distinct sub-processes: the Sketch Generation and the Appearance Transfer processes.

Sketch Generation Process. First, we send the target text prompt as **Text Guidance** to U to start a normal text-guided image generation process, and we interrupt the text-guided generation process at a timestep t and regard the obtained intermediate latent at t as the coarse sketch latent x_t . This sketch latent encapsulates the original inherent text-following capability of the text-to-image model, defining the overall semantic, structure, and color pattern of the image without interference from subject features, as shown by the rightmost image in the **orange** box in Fig. 4.

Appearance Transfer Process. Second, in the rest of the denoising steps, as shown in the **blue** box in Fig. 4, we bring in subject feature \mathcal{F}^{sub} as **Subject Guidance** and transfer the subject appearance to the sketch latent using the trained adapters. Intuitively, we consider that the attention mechanism within each adapter A_n first establishes matching (represented by the attention map) between subject image patches s_n and the noisy sketch latent x_n , and then transfers the content (encoded by the V values) from the subject patches to their corresponding locations in the sketch latent. This understanding can be illustrated in Fig. 4, given the rough sketch x_t from the Sketch Generation Process containing the overall semantic of “a dog in hero’s suit”, our model will first match between the subject dog and the dog in the sketch latent, then transfer only the paired areas and maintain the hero’s suit untouched.

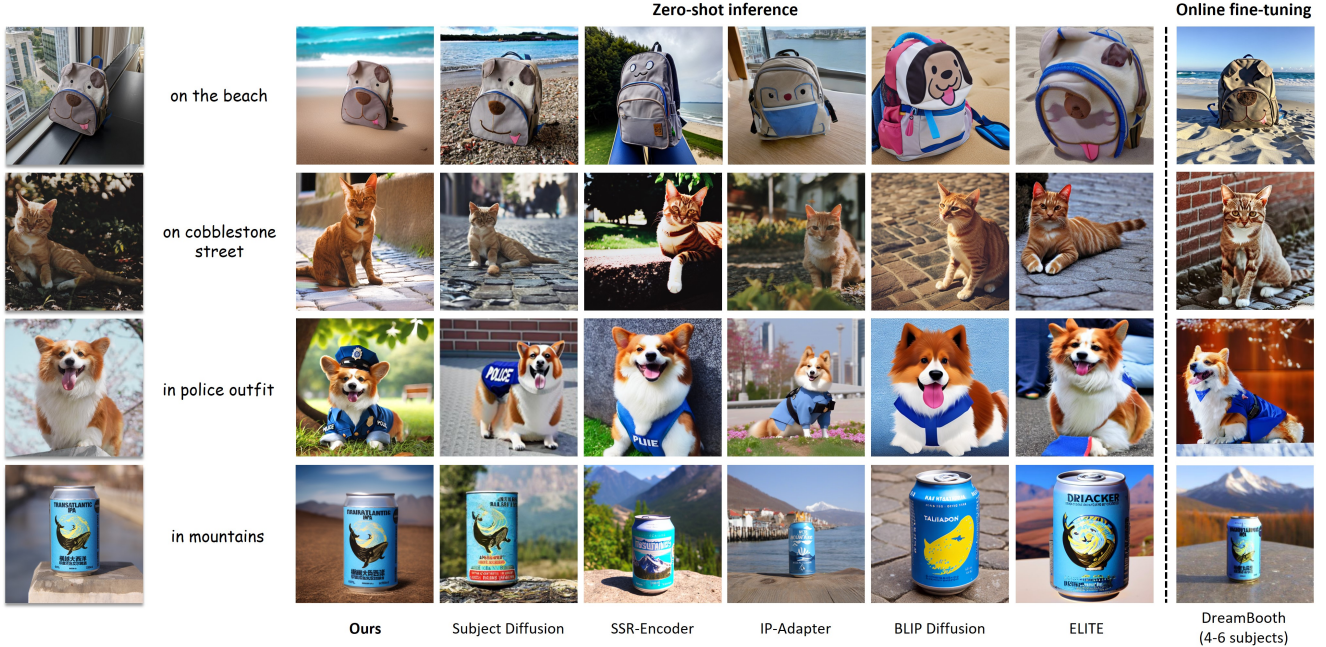


Figure 5. Comparison with existing personalized image generation methods. Our design perfectly preserves the subject’s fine-grained details (e.g. fur textures, body shape, subject structures) while precisely inheriting the flexibilities (e.g. pose variation) from text-prompt.

3.3. Iterative Appearance Transfer

Based on the above analysis and empirical results, we observe that when the sketch latent x_t and the subject share similar semantics, such as rough color patterns, the appearance transfer process improves as the adapter establishes a stronger matching within the UNet’s noisy latent space and could thus transfer more subject appearances. To enhance this, we introduce an iterative generation scheme: when we obtain the clean latent x_0 after the Appearance Transfer Process, we add noise with level t to x_0 to obtain a new x_t as the editable sketch latent for another round of the Appearance Transfer Process, as shown in the bottom part of Fig. 4. This process repeats until the similarity between the newly generated image and the previous image exceeds a predefined threshold, indicating that the appearance transfer is complete and no further information is added. Integrating the designs above, our model successfully balances subject identity preservation and text adherence, ensuring comprehensive guidance-adhering without compromise.

3.4. Zero-shot personalized image editing

We discover that the Appearance Transfer Process can naturally function as an effective zero-shot personalized image editor. This is achieved by integrating an object mask and replacing noise addition with image inversion [27], which converts the generated image back into the sketch latent, preserving the background. Specifically, similar to the noise addition described in Sec. 3.3, given a clean to-edit source image latent x_0 , we first partially invert it based on timestep

t to obtain the coarse sketch latent x_t . Next, we initiate the Appearance Transfer Process to inject the subject feature, resulting in an incomplete edited latent \hat{x}_0 . To ensure an unchanged background, before the next iteration starts, we update \hat{x}_0 extract the edited foreground from \hat{x}_0 and combine it with the static clean background from x_0 using a user-provided mask M :

$$\hat{x}_0 = M \otimes \hat{x}_0 + (1 - M) \otimes x_0 \quad (5)$$

Here, the new \hat{x}_0 combines both the static background and the desired edition result in the foreground, we can then use \hat{x}_0 as the starting point for the next iteration.

4. Experiment

4.1. Implementation details

Benchmark and evaluation. We mainly evaluate EZI-Gen on two standard benchmarks: DreamBench [32] for personalized image generation, DreamEdit [22] for personalized image editing. For both tasks, we follow Subject Diffusion’s protocol, averaging scores over 6 random runs. Regarding the evaluation metric, we report CLIP-T and DINO scores to assess text adherence and subject identity on DreamBench and we evaluate DINO-sub for foreground subject similarities on DreamEditBench, using SAM [18] for mask extraction. We abandon the traditional CLIP-I scores and regard the DINO score as the main metric for subject similarity, as they better depict the detailed patch-level differences between images and are more sensitive to subject quality degradation, as discussed in [32, 38], please



Figure 6. Results on zero-shot personalized image editing task. Our method preserves perfect subject details compared to others.

refer to Appendix C for details. Besides standard evaluation, we additionally validate EZIGen on the challenging human content generation benchmark [40] to test the ability to generalize to domain-specific generation tasks, which usually require special design or in-domain training while EZIGen does not. We report ID preservation and prompt consistency following [28, 40]. At last, we involve human evaluation for the comparisons mentioned above, the percentage scores denote the frequency of the methods’ generation results being chosen as the best within the given sample batch under specific criteria.

Training dataset construction. We create training pairs from COCO2014 and YoutubeVIS. In COCO2014, 1-4 objects are cropped from the target image as subject images, while in YoutubeVIS, we extract images of the same subject from different frames as pairs, following [7]. We sampled 100k pairs from each dataset, totaling 200k pairs. Please refer to Fig. 10 for more details and dataset visualization.

Experiment settings. For a fair comparison, we utilize SD2.1-base as the base model, with an image resolution of 512×512. The adapter is initialized from the self-attention module within each transformer block to enhance compatibility. We train the model for 1 epoch using a batch size of 1, with the Adam optimizer and a learning rate of $1e-5$. During inference, iterations are designed to stop automatically when the newly generated image exhibits a sufficiently high similarity with the image from the previous loop, ensuring efficient convergence and maintaining generation quality. Please refer to Appendix B for more details.

4.2. Method comparisons on DreamBench dataset

In Tab. 1 and Fig. 5, we compare our method with existing zero-shot personalized image generation approaches on the DreamBench dataset [32], including tuning-based methods for reference. We also present the number of reference images required for each subject and the training dataset size to highlight the cost of each method. The results show

Method	CLIP-T	DINO	# Sub	Flex.	ID	Overall Quality
Textual Inv.	0.261	0.561	3-6	3.1%	2.2%	1.1%
DreamBooth	0.306	0.672	4-6	15.4%	17.3%	22.2%
Elite	0.296	0.647	1	6.9%	7.4%	9.0%
BLIP-Diff.	0.298	0.589	1	12.3%	2.7%	2.3%
IP-Adapter	0.274	0.608	1	11.2%	9.1%	6.9%
SSR-Enc.	0.308	0.612	1	20.7%	15.1%	18.4%
BootPIG	0.311	0.674	4-6	-	-	-
Subject Diff.	0.293	0.711	1	-	-	-
Ours	0.316	0.718	1	30.4%	46.2%	40.1%

Table 1. **Left:** Quantitative results on DreamBench. **Right:** Human evaluation results. “# Sub” indicates the number of subject images required for training and inference, “Flex.” and “ID” abbreviate for flexibilities of the generated image and subject identity preservation quality. Our method achieves the highest performance in both quantitative and user studies and also the best balance for both text and subject among all compared approaches.

that our base model achieves state-of-the-art performance text-following, subject identity preservation, and balance among all methods. Compared to the previous state-of-the-art, Subject Diffusion [28], our model outperforms in both CLIP-T (0.316 vs. 0.293) and DINO score (0.718 vs. 0.711), demonstrating superior flexibility in generated images and higher subject identity preservation, without sacrificing balance. Moreover, this was accomplished with $100\times$ less training data, which we attribute to our simplified design and the use of the original Stable Diffusion UNet. These results highlight the advantages of using a Stable Diffusion UNet over CLIP for feature extraction, alongside our decoupling design that improves text coherence. When compared with BootPIG [30], our method surpasses it in text-following ability (0.316 vs. 0.311) and significantly outperforms in DINO score (0.718 vs. 0.674), while requiring fewer subject images. This is due to our effective utilization of the Stable Diffusion UNet extractor. Additionally, our method outperforms previous open-source zero-shot methods [20, 39] across all evaluation metrics.

4.3. Validation on personalized image editing task

As outlined in Sec. 3.4, our method adapts well to personalized image editing by replacing noise addition with image inversion [27] in the Appearance Transfer Process. We compare our

Method	DINO sub	Overall Quality
DreamBooth	0.640	20.3%
PhotoSwap	0.494	11.5%
DreamEdit	0.627	17.1%
MimicBrush	0.642	19.2%
Ours	0.650	31.9%

Table 2. **Left:** Quantitative comparison on personalized image editing task, demonstrating the subject encoder’s ability to provide high-fidelity subject features. **Right:** Human preferences of the overall quality.

We compare our model against previous state-of-the-art methods on the DreamEdit benchmark, as shown in Tab. 2 and Fig. 6. Our method significantly outperforms others, primarily



Figure 7. Qualitative result of the ablation study.

	Full Injection	Decoupled Generation	Iterative App. Trans.	CLIP-T	DINO
1)				0.327	0.362
2)	✓			0.286	0.762
3)	✓	✓		0.321	0.560
4)	✓	✓	✓	0.316	0.718

Table 3. Quantitative ablation study on DreamBench dataset.

due to our advanced subject feature utilization, where the original Stable Diffusion UNet produces high-quality, detailed intermediate appearance features, and the adapter accurately matches them to the sketch latent. Notably, even though MimicBrush [6] leverages a tuned Reference UNet and an extra CLIP image encoder for fine-grained feature extraction, it sometimes struggles to modify areas with large semantic differences from their surroundings. For example, in the last column of Fig. 6, the model has difficulty adjusting the dog face in contrast to the astronaut suit. We attribute this limitation to their masked image modeling training strategy, which aims to recover masked areas based on neighboring tokens.

4.4. Ablation study

We conducted ablation studies to evaluate the effects of various components in our method on DreamBench, including the performance of full-step subject encoding and injecting, the naive Appearance Transfer, and the Iterative Appearance Transfer process, as shown in Tab. 3 and Fig. 7.

Effectiveness of our subject encoder. To evaluate the quality of the encoded subject feature, we start with a fully noised sketch latent (i.e. random noise) and apply subject guidance at all timesteps, dubbed as “full injection”. As shown in Tab. 3 experiments 1) and 2), compared to the original text-guided generation, the encoded subject representation resembles the subject effectively, achieving a DINO score of 0.762. However, the strong subject features override the weaker sketch latent in early timesteps, leading to severe copy-paste effects and a low CLIP-T score of 0.286.

Decoupling the generation process. The experiment in Tab. 3 line 3) confirms the effectiveness of separating the



Figure 8. Visualization of subject ID preservation performance under various UNet configurations.

#ID	Train SDU	Denoise Timestep	DINO
1) BootPIG*	✓	Adaptive	0.589
2)	✗	Adaptive	0.615
3)	✓	$t^{\text{sub}}=1$	0.668
4)	✗	$t^{\text{sub}}=800$	0.427
5)	✗	$t^{\text{sub}}=500$	0.598
6)	✗	$t^{\text{sub}}=300$	0.661
7)	✗	$t^{\text{sub}}=100$	0.725
8) Ours	✗	$t^{\text{sub}}=1$	0.762

Table 4. Scores evaluating subject ID preservation under different SDU configurations. The best result is obtained by using the fixed SDU and using a small denoising timestep t^{sub} . “BootPIG*” indicates BootPIG’s training strategy.

Sketch Generation Process from Appearance Transfer, in which the CLIP-T score improves significantly from 0.286 to 0.321, as this design explicitly maintains the sketch from text prompt. However, when there is a large semantic discrepancy between the sketch latent and the subject, the appearance transfer can be incomplete, resulting in reduced subject similarity scores (0.560) compared to experiment 1).

Effectiveness of Iterative Appearance Transfer. Experiment 4) demonstrates complete appearance transfer after introducing the iterative process. This gentle refinement of the incomplete generated image significantly enhances subject appearance similarity: the DINO score from 0.560 to 0.718. Although the iterative process slightly disrupts text-guided semantics, with the CLIP-T score marginally dropping from 0.321 to 0.316, our model achieves the best balance between the two forms of guidance in this setting.

4.5. Comparing feature extractor with other choices

We evaluate the effectiveness and efficiency of our subject extraction compared to CLIP, DINO, and Reference UNet based methods — Subject Diffusion [28], AnyDoor [7], and BootPIG [30]—as the current best practices for each feature extraction paradigm respectively. For fair comparisons, we ablate the models for AnyDoor and Subject Diffusion (lines 2 and 4) so that subject information is derived solely from the feature extractor. We denote Stable Diffusion UNet, our base extractor, as SDU for simplicity.

Comparing with CLIP- and DINO-based methods. First, to evaluate the efficiency of using SDU versus CLIP and DINO, we directly replaced our “SDU + adapter” combination with “CLIP/DINO + Projector + adapter” and compared performances under identical training settings. As



Figure 9. Comparison with CLIP-based[28] and DINO-based[7] methods. Our method preserves the facial features and expression of the subject dog with greater accuracy, capturing more fur details and providing enhanced flexibility in adapting to the prompt, avoiding the copy-paste effect in Subject Diffusion and AnyDoor.

Subject Encoder	Training Strategies	DINO	Dataset Size
DINO	1) DINO + Projector	0.421	0.2M
	2) AnyDoor <i>w/o high-freq map</i>	0.710	~9M
CLIP	3) CLIP + Projector	0.433	0.2M
	4) Subject Diff. <i>w/o image CLS token</i>	0.637	~76M
Fixed SDU	5) Ours <i>w/full injection</i>	0.762	0.2M

Table 5. Comparing subject encoders, our method is the most efficacious, achieving the highest quality with minimal data requirements. SDU denotes Stable Diffusion UNet.

shown in Tab. 5 lines (1) and (3), this replacement led to trivial solutions, as the adapter struggled to establish attention between misaligned feature maps, causing the model to rely primarily on the text prompt for reconstruction. To address this, additional regularization is typically required to overcome feature space misalignment and force the model to follow the subject guidance. For example, Subject Diffusion employs location control as regularization, while AnyDoor replaces text tokens with image tokens and crops a scene image for the subject feature to fill. However, even with regularization, the required dataset sizes remain substantial, at approximately 76M and 9M image pairs, respectively. In contrast, with closer feature spaces, our method completes training with only 0.2M image pairs. Second, to validate the effectiveness of our design over CLIP and DINO extractors in encoding subject information, we report the DINO scores on the DreamBench dataset using the same evaluation protocol, as shown in Tab. 5 lines (2) and (4), and Fig. 9, the naive SDU extractor significantly outperforms both DINO- and CLIP-based configurations. This suggests that, although CLIP and DINO are highly effective for high-fidelity image representation across various downstream tasks [25, 36, 43], the SDU is naturally more suitable for providing features for high-quality image generation.

Evaluating alternative feature extractor configurations.

We examined the impact of tuning SDU parameters and adding varying levels of noise to subject images. Tab. 4 lists the experiment settings and their performances, where check marks/cross marks indicate whether the SDU extractor is trained or frozen, the corresponding visualization re-

Method	ID Preser.	Prompt Consis.	ID Preser.	Prompt Consis.	Overall Quality
DreamBooth	0.273	0.239	21.7%	20.6%	20.3%
FastComposer	0.514	0.243	36.5%	45.2%	37.5%
SubjectDiffusion	0.605	0.228	-	-	-
Ours	0.598	0.237	41.8%	34.1%	42.2%

Table 6. **Left:** Quantitative evaluation following [40]. **Right:** Human preferences for each metric and the overall generation quality. EZIGen shows very competitive results in domain-specific generation tasks **WITHOUT** using domain-specific datasets or large-scale pre-training, it also achieves a perfect balance between ID preservation and prompt consistency. These results further highlight our design, reaching high in both aspects without sacrifices.

sults are shown in Fig. 8. “Adaptive” means that the tuned SDU extractor shares the same denoising timestep as the main SDU, while arguments starting with “ t^{sub} ” indicate the level of noise we add to the subject image. From lines (1) and (2), we find that tuning the SDU disrupts the original generative capabilities of the SDU, resulting in a performance drop compared to freezing it. Lines (1) and (3) show that fixing the denoising timestep of the SDU to a small t^{sub} produces better subject identity with clearer feature maps. By fixing the SDU and adjusting t^{sub} , we validated its importance; as shown in lines (4) to (8), subject identity scores increase as t^{sub} decreases. This aligns with the intuition that the SDU encodes clearer features in the final timesteps of the generation process.

4.6. Zero-shot abilities for domain-specific task

To demonstrate the versatility of our model, we further evaluate the effectiveness of our method for a domain-specific generation task, namely personalized human image generation. Compared to generating common objects, producing accurate human faces is extremely challenging as human brains possess strong overfittings to human facial landmarks, making even the slightest distortion prominent. We report the performance following FastComposer’s evaluation protocols and report the results in Tab. 6 and Fig. 14 in the appendix. Unlike FastComposer[40], which relies on domain-specific datasets, or Subject Diffusion [28], which requires large-scale pretraining, our model achieves high-quality results using only a normal-scale open-domain dataset. As shown in Tab. 6, our approach delivers very competitive results. Regarding subject ID preservation, we match Subject Diffusion and outperform FastComposer. While our prompt consistency lags behind FastComposer and DreamBooth, it still exceeds Subject Diffusion. These findings further prove the capabilities of EZIGen in capturing fine-grained subject details regardless of categories.

5. Conclusion

In conclusion, EZIGen effectively addresses the challenges of zero-shot personalized image generation by balancing subject identity preservation and text adherence. Through a

carefully designed subject image encoder and a novel guidance separation strategy, it achieves state-of-the-art performance on multiple benchmarks with significantly reduced training data, demonstrating its efficiency and versatility.

References

- [1] Omri Avrahami, Kfir Aberman, Ohad Fried, Daniel Cohen-Or, and Dani Lischinski. Break-a-scene: Extracting multiple concepts from a single image. In *SIGGRAPH Asia 2023 Conference Papers*, pages 1–12, 2023. 1
- [2] Omri Avrahami, Amir Hertz, Yael Vinker, Moab Arar, Shlomi Fruchter, Ohad Fried, Daniel Cohen-Or, and Dani Lischinski. The chosen one: Consistent characters in text-to-image diffusion models. In *ACM SIGGRAPH 2024 Conference Papers*, pages 1–12, 2024. 3
- [3] James Betker, Gabriel Goh, Li Jing, Tim Brooks, et al. Improving image generation with better captions. Technical report, OpenAI, 2023. 3
- [4] Andrew Brock, Jeff Donahue, and Karen Simonyan. Large scale gan training for high fidelity natural image synthesis. *arXiv preprint arXiv:1809.11096*, 2018. 2
- [5] Hong Chen, Yipeng Zhang, Simin Wu, Xin Wang, Xuguang Duan, Yuwei Zhou, and Wenwu Zhu. Disenbooth: Identity-preserving disentangled tuning for subject-driven text-to-image generation. *arXiv preprint arXiv:2305.03374*, 2023. 3
- [6] Xi Chen, Yutong Feng, Mengting Chen, Yiyang Wang, Shilong Zhang, Yu Liu, Yujun Shen, and Hengshuang Zhao. Zero-shot image editing with reference imitation. *arXiv preprint arXiv:2406.07547*, 2024. 2, 3, 7
- [7] Xi Chen, Lianghua Huang, Yu Liu, Yujun Shen, Deli Zhao, and Hengshuang Zhao. Anydoor: Zero-shot object-level image customization. In *Proceedings of the IEEE/CVF Conference on Computer Vision and Pattern Recognition*, pages 6593–6602, 2024. 1, 2, 3, 6, 7, 8
- [8] Prafulla Dhariwal and Alexander Nichol. Diffusion models beat gans on image synthesis. *Advances in neural information processing systems*, 34:8780–8794, 2021. 3
- [9] Yuxuan Ding, Chunna Tian, Haoxuan Ding, and Lingqiao Liu. The clip model is secretly an image-to-prompt converter. *Advances in Neural Information Processing Systems*, 36, 2024. 3
- [10] Patrick Esser, Robin Rombach, and Bjorn Ommer. Taming transformers for high-resolution image synthesis. In *Proceedings of the IEEE/CVF conference on computer vision and pattern recognition*, pages 12873–12883, 2021. 3
- [11] Rinon Gal, Yuval Alaluf, Yuval Atzmon, Or Patashnik, Amit H Bermano, Gal Chechik, and Daniel Cohen-Or. An image is worth one word: Personalizing text-to-image generation using textual inversion. *arXiv preprint arXiv:2208.01618*, 2022. 1, 3
- [12] Ian Goodfellow, Jean Pouget-Abadie, Mehdi Mirza, Bing Xu, David Warde-Farley, Sherjil Ozair, Aaron Courville, and Yoshua Bengio. Generative adversarial networks. *Communications of the ACM*, 63(11):139–144, 2020. 2
- [13] Shaozhe Hao, Kai Han, Shihao Zhao, and Kwan-Yee K Wong. Vico: Plug-and-play visual condition for personalized text-to-image generation. 2023. 1, 3
- [14] Jonathan Ho, Ajay Jain, and Pieter Abbeel. Denoising diffusion probabilistic models. *Advances in neural information processing systems*, 33:6840–6851, 2020. 3
- [15] Li Hu. Animate anyone: Consistent and controllable image-to-video synthesis for character animation. In *Proceedings of the IEEE/CVF Conference on Computer Vision and Pattern Recognition*, pages 8153–8163, 2024. 2, 3
- [16] Tero Karras, Miika Aittala, Samuli Laine, Erik Härkönen, Janne Hellsten, Jaakko Lehtinen, and Timo Aila. Alias-free generative adversarial networks. *Advances in neural information processing systems*, 34:852–863, 2021. 2
- [17] Diederik P Kingma and Max Welling. Auto-encoding variational bayes. *arXiv preprint arXiv:1312.6114*, 2013. 2
- [18] Alexander Kirillov, Eric Mintun, Nikhila Ravi, Hanzi Mao, Chloe Rolland, Laura Gustafson, Tete Xiao, Spencer Whitehead, Alexander C Berg, Wan-Yen Lo, et al. Segment anything. In *Proceedings of the IEEE/CVF International Conference on Computer Vision*, pages 4015–4026, 2023. 5
- [19] Nupur Kumari, Bingliang Zhang, Richard Zhang, Eli Shechtman, and Jun-Yan Zhu. Multi-concept customization of text-to-image diffusion. In *Proceedings of the IEEE/CVF Conference on Computer Vision and Pattern Recognition*, pages 1931–1941, 2023. 1, 3
- [20] Dongxu Li, Junnan Li, and Steven Hoi. Blip-diffusion: Pre-trained subject representation for controllable text-to-image generation and editing. *Advances in Neural Information Processing Systems*, 36, 2024. 1, 2, 3, 6
- [21] Junnan Li, Dongxu Li, Silvio Savarese, and Steven Hoi. Blip-2: Bootstrapping language-image pre-training with frozen image encoders and large language models. In *International conference on machine learning*, pages 19730–19742. PMLR, 2023. 3
- [22] Tianle Li, Max Ku, Cong Wei, and Wenhui Chen. Dreamedit: Subject-driven image editing, 2023. 5
- [23] Zhen Li, Mingdeng Cao, Xintao Wang, Zhongang Qi, Ming-Ming Cheng, and Ying Shan. Photomaker: Customizing realistic human photos via stacked id embedding. In *Proceedings of the IEEE/CVF Conference on Computer Vision and Pattern Recognition*, pages 8640–8650, 2024. 3
- [24] Tsung-Yi Lin, Michael Maire, Serge Belongie, James Hays, Pietro Perona, Deva Ramanan, Piotr Dollár, and C Lawrence Zitnick. Microsoft coco: Common objects in context. In *Computer Vision—ECCV 2014: 13th European Conference, Zurich, Switzerland, September 6–12, 2014, Proceedings, Part V 13*, pages 740–755. Springer, 2014. 1
- [25] Haotian Liu, Chunyuan Li, Qingyang Wu, and Yong Jae Lee. Visual instruction tuning. *Advances in neural information processing systems*, 36, 2024. 8
- [26] Zhiheng Liu, Yifei Zhang, Yujun Shen, Kecheng Zheng, Kai Zhu, Ruili Feng, Yu Liu, Deli Zhao, Jingren Zhou, and Yang Cao. Cones 2: Customizable image synthesis with multiple subjects. In *Proceedings of the 37th International Conference on Neural Information Processing Systems*, pages 57500–57519, 2023. 3

- [27] Shilin Lu, Yanzhu Liu, and Adams Wai-Kin Kong. Tf-icon: Diffusion-based training-free cross-domain image composition. In Proceedings of the IEEE/CVF International Conference on Computer Vision, pages 2294–2305, 2023. [1](#), [2](#), [3](#), [4](#), [6](#), [5](#), [6](#)
- [28] Jian Ma, Junhao Liang, Chen Chen, and Haonan Lu. Subject-diffusion: Open domain personalized text-to-image generation without test-time fine-tuning. arXiv preprint arXiv:2307.11410, 2023. [1](#), [2](#), [3](#), [4](#), [6](#), [7](#), [8](#)
- [29] Jisu Nam, Heesu Kim, DongJae Lee, Siyoon Jin, Seungryong Kim, and Seunggyu Chang. Dreammatcher: Appearance matching self-attention for semantically-consistent text-to-image personalization. In Proceedings of the IEEE/CVF Conference on Computer Vision and Pattern Recognition, pages 8100–8110, 2024. [3](#)
- [30] Senthil Purushwalkam, Akash Gokul, Shafiq Joty, and Nikhil Naik. Bootpig: Bootstrapping zero-shot personalized image generation capabilities in pretrained diffusion models. arXiv preprint arXiv:2401.13974, 2024. [1](#), [2](#), [3](#), [4](#), [6](#), [7](#)
- [31] Ali Razavi, Aaron Van den Oord, and Oriol Vinyals. Generating diverse high-fidelity images with vq-vae-2. Advances in neural information processing systems, 32, 2019. [3](#)
- [32] Nataniel Ruiz, Yuanzhen Li, Varun Jampani, Yael Pritch, Michael Rubinstein, and Kfir Aberman. Dreambooth: Fine tuning text-to-image diffusion models for subject-driven generation. In Proceedings of the IEEE/CVF Conference on Computer Vision and Pattern Recognition, pages 22500–22510, 2023. [1](#), [3](#), [5](#), [6](#), [2](#)
- [33] Jing Shi, Wei Xiong, Zhe Lin, and Hyun Joon Jung. Instantbooth: Personalized text-to-image generation without test-time finetuning. In Proceedings of the IEEE/CVF Conference on Computer Vision and Pattern Recognition, pages 8543–8552, 2024. [3](#)
- [34] Jiaming Song, Chenlin Meng, and Stefano Ermon. Denoising diffusion implicit models. arXiv preprint arXiv:2010.02502, 2020. [3](#)
- [35] Peize Sun, Yi Jiang, Shoufa Chen, Shilong Zhang, Bingyue Peng, Ping Luo, and Zehuan Yuan. Autoregressive model beats diffusion: Llama for scalable image generation. arXiv preprint arXiv:2406.06525, 2024. [3](#)
- [36] Quan Sun, Yufeng Cui, Xiaosong Zhang, Fan Zhang, Qiyang Yu, Yueze Wang, Yongming Rao, Jingjing Liu, Tiejun Huang, and Xinlong Wang. Generative multimodal models are in-context learners. In Proceedings of the IEEE/CVF Conference on Computer Vision and Pattern Recognition, pages 14398–14409, 2024. [8](#)
- [37] Keyu Tian, Yi Jiang, Zehuan Yuan, Bingyue Peng, and Liwei Wang. Visual autoregressive modeling: Scalable image generation via next-scale prediction. arXiv preprint arXiv:2404.02905, 2024. [3](#)
- [38] X Wang, Siming Fu, Qihan Huang, Wangui He, and Hao Jiang. Ms-diffusion: Multi-subject zero-shot image personalization with layout guidance. arXiv preprint arXiv:2406.07209, 2024. [3](#), [5](#), [2](#)
- [39] Yuxiang Wei, Yabo Zhang, Zhilong Ji, Jinfeng Bai, Lei Zhang, and Wangmeng Zuo. Elite: Encoding visual concepts into textual embeddings for customized text-to-image generation. In Proceedings of the IEEE/CVF International Conference on Computer Vision, pages 15943–15953, 2023. [1](#), [2](#), [3](#), [4](#), [6](#)
- [40] Guangxuan Xiao, Tianwei Yin, William T Freeman, Frédo Durand, and Song Han. Fastcomposer: Tuning-free multi-subject image generation with localized attention. arXiv preprint arXiv:2305.10431, 2023. [3](#), [6](#), [8](#)
- [41] Linjie Yang, Yuchen Fan, Yang Fu, and Ning Xu. The 3rd large-scale video object segmentation challenge - video instance segmentation track, 2021. [1](#)
- [42] Yuxuan Zhang, Yiren Song, Jiaming Liu, Rui Wang, Jinpeng Yu, Hao Tang, Huaxia Li, Xu Tang, Yao Hu, Han Pan, et al. Ssr-encoder: Encoding selective subject representation for subject-driven generation. In Proceedings of the IEEE/CVF Conference on Computer Vision and Pattern Recognition, pages 8069–8078, 2024. [3](#)
- [43] Ziqin Zhou, Yinjie Lei, Bowen Zhang, Lingqiao Liu, and Yifan Liu. Zegclip: Towards adapting clip for zero-shot semantic segmentation. In Proceedings of the IEEE/CVF Conference on Computer Vision and Pattern Recognition, pages 11175–11185, 2023. [8](#)

EZIGen: Enhancing zero-shot personalized image generation with precise subject encoding and decoupled guidance

Supplementary Material



Figure 10. Exemplary training image pairs from the source datasets.

Number of loops	CLIP-T	DINO
0	0.321	0.560
1	0.317	0.627
5	0.316	0.694
10	0.308	0.720
Auto-stop (avg. 6.67)	0.316	0.718

Table 7. Evaluating subject-driven image generation task on DreamBench dataset with different iterative loops. The performance of the auto-stop mechanism reaches the best balance between subject identity and text following, resulting in 6.67 average steps for each evaluation pair on the DreamBench dataset.

A. Dataset construction

The training dataset is constructed using two widely recognized datasets: COCO2014[24] and YoutubeVIS[41], examples are illustrated in Fig. 10.

COCO2014 Dataset. We crop 1 to 4 objects from a given target image to serve as the subject images. Each cropped

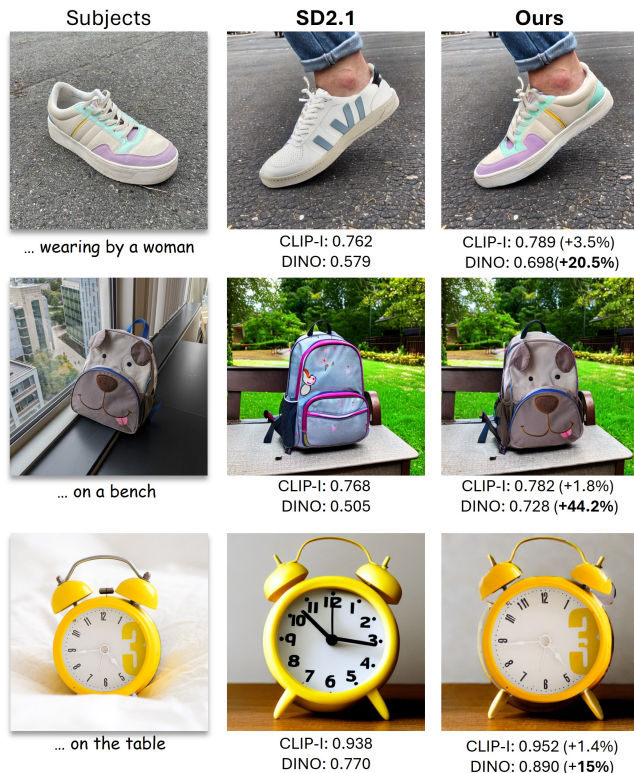


Figure 11. Comparing the sensitivity of DINO and CLIP-I scores on subject appearance changes. To avoid disturbance, we fix all other variables such as image layout, subject size, pose, and background by generating our target images using EZIGen’s editing mode based on the results from the Stable Diffusion 2.1 base, and thus the score would only reflect the foreground detailed texture changes.

object, along with the corresponding full image, forms a subject-target training pair. This pairing ensures that the model learns the association between individual subjects and the broader scene in which they are located.

YoutubeVIS Dataset. The YoutubeVIS dataset contains videos with annotated instances of objects over time. To create training pairs, we extract images of the same subject from different frames of a video, following the methodology proposed in [7]. This process captures the variations in appearance, pose, and position of the same subject across different frames, providing valuable temporal data that helps the model learn consistent subject identification even in dynamic scenes.

Method	CLIP-T	DINO	# Sub	TS	DS	ZS
Textual Inversion	0.261	0.561	3-6	N/A	N/A	✗
DreamBooth	0.306	0.672	4-6	N/A	N/A	✗
Elite	0.296	0.647	1	multi	0.125M	✓
BLIP-Diffusion	0.298	0.589	1	multi	~2M	✓
IP-Adapter	0.274	0.608	1	single	10M	✓
SSR-Encoder	0.308	0.612	1	single	10M	✓
BootPIG	0.311	0.674	4-6	single	0.2M	✓
Subject Diffusion	0.293	0.711	1	single	~76M	✓
Ours	0.316	0.718	1	single	0.2M	✓

Table 8. More quantitative comparisons on DreamBench. For each abbreviation, “#Sub” stands for the number of subject images required, and “TS” indicates if the methods are trained end-to-end or require multiple stages of pertaining. “DS” represents the dataset size required for achieving the reported scores, and “ZS” shows if the method is capable of zero-shot inference. Our method achieves the most satisfying results with the least system complexity compared to previous methods.



Figure 12. This figure showcases the falsity of the CLIP-I score on evaluating subject similarity. The CLIP-I score measures more overall image semantics rather than local image details, therefore, when the foreground object shares similar semantics (e.g. “red” backpack) with the subject image and the foreground object occupies a large area of the image frame, CLIP-I tends to falsely report higher scores while DINO score remains aligned with human observations.

B. Autostop mechanism

We use the DINOv2 image encoder as the criteria calculator. For each newly generated image and the image from the previous loop, we calculate patch-wise similarity using the DINOv2 encoder. If the similarity exceeds a predefined threshold, the iterative process stops, indicating sufficient subject feature transfer. To handle cases where the layout image differs significantly from the subject image, leading to weak injection, we enforce a minimum of 3 loops. For difficult cases where feature map similarity remains low, we

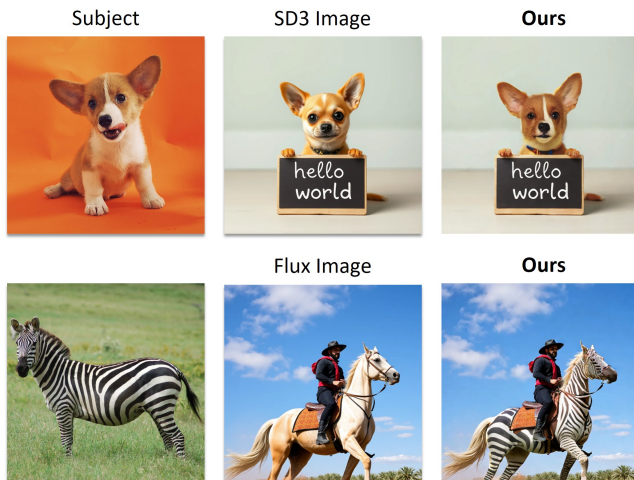


Figure 13. Integration with stronger base image models, namely Flux and Stable Diffusion 3.

cap the maximum loop count at 10. We evaluate performance on the DreamBench dataset with varying loop numbers in Tab. 7.

C. Justify evaluation metric: CLIP-I v.s. DINO

CLIP-I and DINO scores have long been used as evaluation metrics in the field[7, 20, 28, 30, 32, 38, 39], where they calculate the [CLS] embedding similarity between the subject image and the generated target to determine how well the target image ensembles the subject, using CLIP image encoder and DINO respectively. However, we identified potential issues within such settings. Firstly, as discussed in [38], DINO distinguishes fine-grained nuances between the generated image and the given subject reference more effectively, this is illustrated in Fig. 11, when the texture changes, DINO scores fluctuate significantly, while CLIP-I scores show only slight variations. Secondly, we also observe that CLIP-I may sometimes inaccurately report sub-



Figure 14. Comparison on the challenging zero-shot human content generation task. Our method can provide high-quality facial features for generating realistic and ID-preserved human images. The quantitative results are listed in Tab. 6.

ject similarity. As shown in Fig. 12, when compared to SD2.1-base (enhanced with a detailed subject caption), it is clear that our method preserves subject details accurately, whereas the original text-guided generation does not. However, the evaluation scores tell a different story: SD2.1-base achieves a higher CLIP-I score, while the DINO score aligns with our observations despite background changes.

D. User study details

Except for quantitative comparisons, we further evaluate our methods based on human preferences. These results are listed in Tab. 1, Tab. 2 and Tab. 6. Specifically, for each evaluation metric, human evaluators select their preferred images the best match indicated evaluation metric from batches of shuffled images generated by each competing method. The preferences are then aggregated across batches to calculate the percentages reported in each table.

E. Integrating with existing T2I generators

E.1. Training free integration

Despite the fact that the method is developed based on Stable Diffusion 2.1 base, it could be naturally integrated with existing state-of-the-art base models. For instance, in Fig. 13, we regard our EZIGen model as a subject-driven image editor and replace the specific concepts within the

original image generated by advanced image models such as Stable Diffusion 3 and Flux models.

E.2. Training on advanced base models

We also empirically presume that our concept and designs are suitable for tuning all diffusion- or flow-matching-based models as they all share a similar add-noise/denoising process as Stable Diffusion 2.1, therefore, we believe that with proper datasets and base-model-related structure modifications, the trained models are expected to obtain similar or even better results compared to the current design.

F. Limitations and future work

EZIGen may sometimes fail to generate images containing subjects with drastic pose variations, for example, given an image of a dog facing toward the camera, it would be rather challenging to generate an image with the dog facing forward. Moreover, our model inherits the weakness from Stable Diffusion 2.1 that the model cannot output accurate detailed text characters. Future possibilities for a more advanced model include migrating the subject encoding technique to more advanced image/video base models.

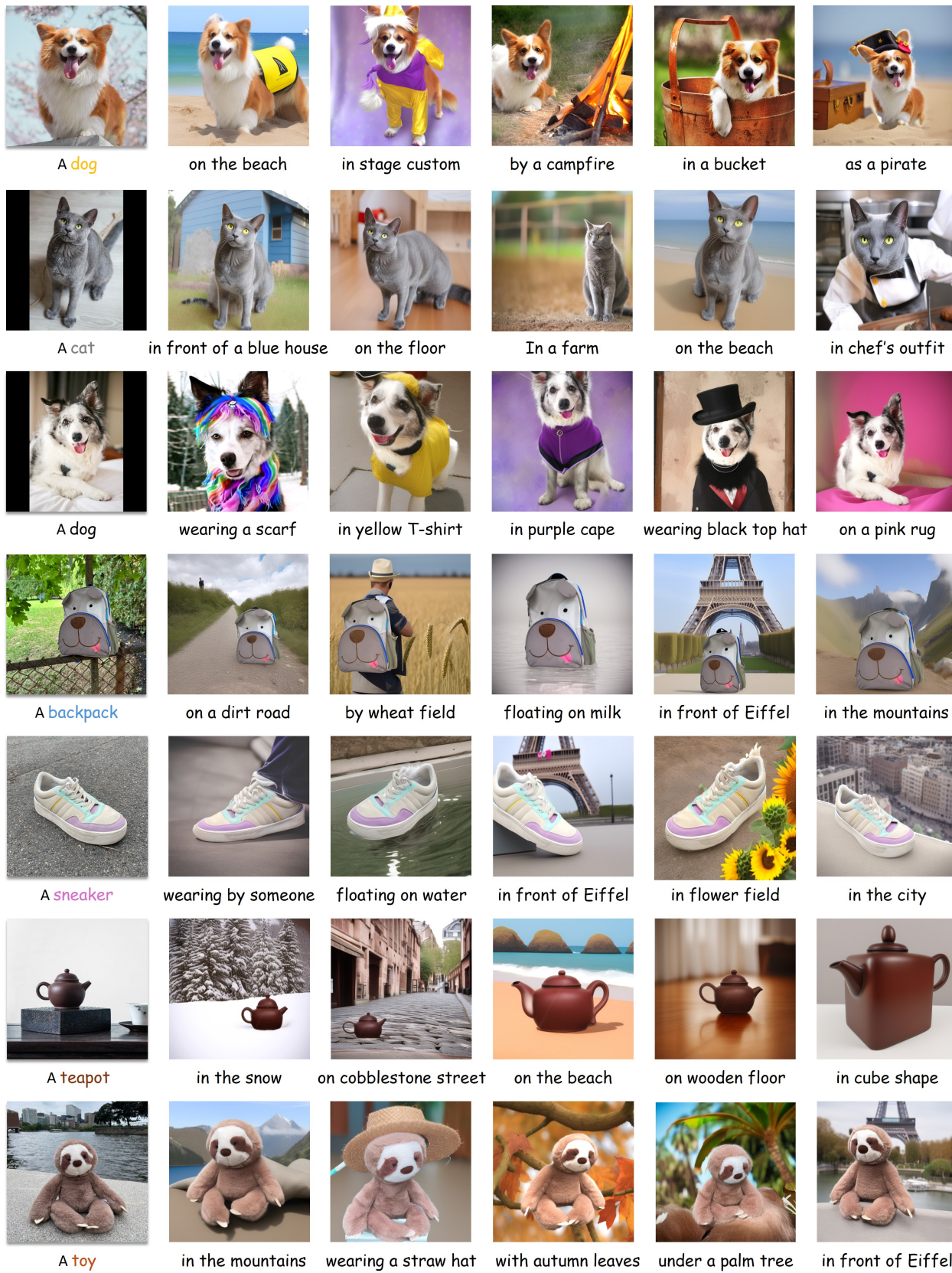


Figure 15. More visualization results for personalized image generation.

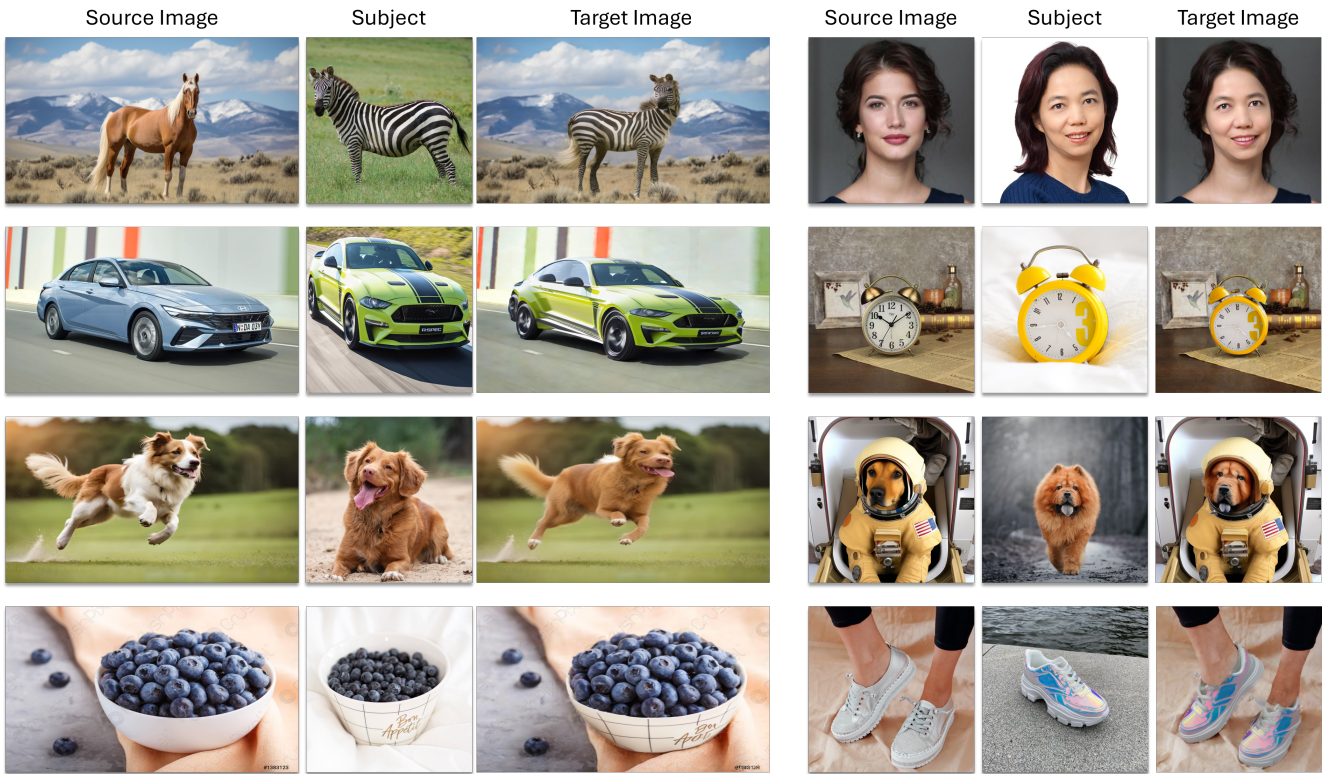


Figure 16. More visualization results for personalized image editing.



Figure 17. Interpolation between subjects.